chemosensors

Article

An Electrochemical Immunosensor with PEDOT: PSS/MWCNTs-COOH Nanocomposites as a Modified Working Electrode Material for Detecting Tau-441

Hanwen Ren [1,2], Xiansu Liu [1], Shanshan Wei [3], Feijun Zhao [1,2], Zhencheng Chen [1,2,3,*] and Haolin Xiao [3,*]

[1] School of Life and Environmental Sciences, Guilin University of Electronic Technology, Guilin 541004, China; 21122202018@mails.guet.edu.cn (H.R.); 22122202009@mails.guet.edu.cn (X.L.); zhaofeijun@guet.edu.cn (F.Z.)
[2] Guangxi Human Physiological Information Non Invasive Detection Engineering Technology Research Center; Guilin 541004, China
[3] School of Electronic Engineering and Automation, Guilin University of Electronic Technology, Guilin 541004, China; shanshanwei66@gmail.com
* Correspondence: chenzhcheng@163.com (Z.C.); xiaohaolin@guet.edu.cn (H.X.)

Abstract: The progression of Alzheimer's disease (AD) is positively correlated with the phosphorylation damage of Tau-441 protein, which is the marker with the most potential for the early detection of AD. The low content of Tau-441 in human serum is a major difficulty for the realization of content detection. Herein, we prepared an electrochemical immunosensor modified with Poly(3,4-ethylenedioxythiophene)-poly (styrene sulfonate) (PEDOT: PSS)/Carboxylated multi-walled carbon nanotube (MWCNTs-COOH) nanocomposites based on electrochemical immunoassay technology for the low-concentration detection of Tau-441. The immunosensor based on the nanocomposite can take advantage of the characteristics of conductive polymers to achieve electrical signal amplification and use MWCNTs-COOH to increase the contact area of the active site and bond with the Tau-441 antibodies on the electrode. The physicochemical and electrical properties of PEDOT: PSS/MWCNTs-COOH were studied by in situ characterization techniques and electrochemical characterization methods, indicating that the immunosensor has high selectivity and sensitivity to the Tau-441 immune reaction. Under optimized optimal conditions, the electrochemical immunosensor detected a range of concentrations of Tau-441 to obtain a low detection of limit (0.0074 ng mL^{-1}) and demonstrated good detection performance through actual human serum sample testing experiments. Therefore, the study provides an effective reference value for the early diagnosis of AD.

Keywords: PEDOT: PSS; MWCNTs-COOH; nanocomposites; electrochemical immunosensor; Tau-441

Citation: Ren, H.; Liu, X.; Wei, S.; Zhao, F.; Chen, Z.; Xiao, H. An Electrochemical Immunosensor with PEDOT: PSS/MWCNTs-COOH Nanocomposites as a Modified Working Electrode Material for Detecting Tau-441. *Chemosensors* **2023**, *11*, 573. https://doi.org/10.3390/chemosensors11120573

Academic Editor: Núria Serrano

Received: 11 October 2023
Revised: 12 November 2023
Accepted: 30 November 2023
Published: 4 December 2023

1. Introduction

Alzheimer's disease (AD) is a progressive neurodegenerative disorder with a long latency period and irreversibility [1,2]. An estimated 6.7 million Americans age 65 and older are currently living with AD. Official death certificates show that Alzheimer's disease is officially listed as the sixth leading cause of death in the United States [3]. The main tools for the clinical diagnosis of AD are the analysis of positron emission tomography images (PET) and the levels of key biomarkers (beta-amyloid, Tau protein) in the cerebrospinal fluid (CSF) [4,5]. These clinical diagnostic methods are expensive and complex, which is the main reason for the low diagnosis rate of AD. Therefore, it is very important to study a portable and low-cost detection method for the early detection of AD patients. So far, the widely used hypotheses on the pathogenesis of AD mainly include the amyloid cascade hypothesis [6,7] and the Tau protein hyperphosphorylation hypothesis [8,9], which are also the principles for detecting AD markers in CSF. The microtubule system is the cytoskeletal component of the nerve. Tau protein, as a microtubule-related protein, binds to microtubules in the normal human brain and has the function of maintaining microtubule

stability. However, the total amount of Tau protein in the brain of AD patients is higher than that of normal people, with a decrease in normal Tau protein and a substantial increase in hyperphosphorylated Tau protein. Microtubule stability is impaired. The abnormal accumulation of Tau protein causes neurofibrillary tangles (NFTs), which lead to the degeneration of neuronal fibers and the onset of dementia in patients. Therefore, Tau protein is an important marker for the diagnosis of AD patients [10–12]. Because the process of obtaining CSF is complex and painful for patients, testing for AD through minimally invasive blood has been a key topic of research for scientists in recent years. At present, a large number of scientific studies have confirmed the relationship between Tau protein in blood and the concentration of Tau protein in CSF [13]. In particular, the relationship between Tau levels in plasma/serum and the disease has provided a lot of evidence for diagnosing AD, so more and more studies have been conducted to diagnose AD based on the biomarker Tau [8,11,14]. The detection of total Tau protein (Tau-441) in human serum not only alleviates the pain of patients but also shortens the detection time and reduces the difficulty of detection. And more importantly, it is conducive to the timely control and treatment of patients' disease. Therefore, achieving low-concentration detection of Tau-441 in serum remains a challenging problem.

The electrochemical detection system has been successfully applied to the highly sensitive quantitative analysis of biological samples because of its high sensitivity and simplicity, and low cost [15–18]. Immunoassay is a method for quantitative analysis by measuring the binding rate of specific recognition sites and has the characteristics of high selectivity, strong specificity, and a low detection limit [19–21]. Electrochemical immunoassay is a potential new tool for the rapid and accurate detection and diagnosis of diseases by combining electrochemical detection and immunoassay. At present, the common means of detection of Tau-441 are enzyme-linked immunosorbent assay (ELISA) [22,23], and surface plasmon resonance (SPR) [24–26]. These methods have lots of shortcomings such as cumbersome operation processes, expensive detection equipment, and a high threshold of application. Therefore, biosensors designed based on electrochemical immunoassay can be used to detect at the single-molecule level due to its simple operation, rapid detection process, and further amplification of electrical signals. A large number of studies have reported that electrochemical immunosensors can be used to detect Tau-441 protein and have widely outstanding detection results because of their simplicity, low cost, and portability [13,27–31].

Recently, conducting polymers have been widely used in biosensors due to their high electrical conductivity. Poly(3,4-ethylene-dioxythiophene)-poly (styrene sulfonic acid) (PEDOT: PSS) has been used more as an electrode modifier for electrochemical sensors because of its good compatibility and high electrical conductivity with metal nanoparticles, polymers, and carbide materials [32,33]. Multi-walled carbon nanotubes (MWCNTs), which can be used as carbon fiber materials, have a stable structure, large specific surface area, high aspect ratio, and strong stability. MWCNTs are often used as electrode modification materials to reduce the overpotential of electrodes, increase the current response, and improve the selectivity and sensitivity of electrodes [34,35]. Multi-walled carbon nanotubes with carboxylic groups (MWCNTs-COOH) have the properties of MWCNTs but also have a much stronger metal chelating ability and improved water solubility. Carboxylic groups (-COOH) can further increase the electron transfer rate, and electrodes modified with -COOH can also stabilize antibodies by covalent bonding. MWCNTs-COOH have better applications in the field of electrochemical immunosensors [35]. The doping of MWCNT-COOH in PEDOT: PSS can improve the conductivity of conductive polymer and provide functional groups that bind to protein antibodies, which greatly improves the application of electrochemical immunosensors.

In this work, we provide an electrochemical immunosensor based on using a polymer PEDOT: PSS and MWCNTs-COOH hybrid composite as an electrochemical immunosensor. The sensor uses Tau-441 antibody as a specific recognition method and electrodeposition modification of the electrode by the composite PEDOT: PSS/MWCNTs-COOH, which is prepared by hybridization of PEDOT: PSS and MWCNTs-COOH with good electrical conductivity and high stability, followed by the quantitative analysis of Tau-441 by electrochemical methods.

In addition, a good result was obtained in the recovery test of the human serum. This work provides a convenient and rapid detection method for the detection of Tau-441 levels.

2. Experimental Methods

2.1. Materials and Reagents

Poly-(styrene sulfonic acid sodium salt) (PSSNa), ammonium persulfate (APS), ethylenedioxythiophene (EDOT), and Poly-(3, 4-ethylene-dioxythiophene)-poly-(styrene sulfonate) (PEDOT: PSS) were purchased from Aladdin Inc. (Shanghai, China). The experimental ingredients acetone, ethanol, hydrochloric acid (HCL), sodium dihydrogen phosphate dihydrate (NaH_2PO_4), disodium hydrogen phosphate dodecahydrate (Na_2HPO_4) and potassium chloride (KCl), used for the preparation of phosphate-buffered solution (PBS) at pH = 7.4, were purchased from Xilong Scientific Company (Shantou, China). Potassium ferricyanide ($K_3Fe(CN)_6$) was purchased from Energy Chemical (Shanghai, China). Carboxyl multi-wall carbon nanotubes (MWCNTs-COOH) (long, 8–15 nm) were obtained from Nanjing XFNANO Materials Tech Co., Ltd. (Nanjing, China). Thionin Acetate (Thi) was purchased from Yuanye Bio-Technology Co., Ltd. (Shanghai, China). Iron(III) chloride hexahydrate ($FeCl_3 \cdot 6H_2O$) was bought from Anhui Sennrise Technology Co., Ltd. (Hefei, China). Bovine serum albumin (BSA), alpha-fetoprotein (AFP), and carcinoembryonic antigen (CEA) were purchased from Sigma-Aldrich Co., Ltd. (St. Louis, MO, USA). Ultrapure water was prepared through a Milli-Q purification system (Milli-Pore, Bedford, MA, USA). Tau-441 protein was bought from ACRO Biosystems Co, Ltd. (Beijing, China) Anti-Tau (39E10, binding sites 186–195) was bought from BioLegend, Inc. (Waltham, MA, USA). Screen-printed electrode (SPE) was provided by Nanjing Yunyou Biotechnology Co., Ltd. (Nanjing, China).

2.2. Apparatus

The morphology and X-ray energy dispersive spectroscopy (EDS) analysis were characterized using a scanning electron microscope (SEM, Tescan Mira4, Brno, Czech). The instrument for obtaining information about chemical bonds was a Fourier-transform infrared spectrometer (FTIR, Thermo Scientific iN10, Waltham, MA, USA). X-ray photoelectron spectroscopy (XPS) was scaled by a Thermo Scientific K-Alpham (USA). All electrochemical detection methods including cyclic voltammetry (CV) and differential pulse voltammetry (DPV) were implemented using a CHI660D electrochemical workstation (Chenhua Instrument Co., Ltd., Shanghai, China).

2.3. Preparation of the Nanocomposite

The nanocomposites were synthesized with some adjustments according to previous reports [36]. The process of preparing nanocomposites is shown in Figure 1A. Firstly, the appropriate amount of MWCNTs-COOH was dispersed in 50 mL of 0.01 mol L^{-1} HCl and then ultrasonicated for 0.5 h. The suspension was treated with cell crusher for 0.5 h. Next, 15 mL of 1 mg mL^{-1} PSSNa aqueous solution was added to the above dispersion. The mixed solution was ultrasonicated for 0.5 h and magnetically stirred at 60 °C for 2 h to form a uniform suspension. After cooling to room temperature, 0.01 mol EDOT was added to the black solution and continuously stirred for 1 h to turn it into a blue-black solution. Then, the mixed solution, which was prepared by adding 0.01 mol APS into 50 mL of 30 mg L^{-1} $FeCl_3$ solution and stirring until completely dissolved, was slowly added into the blue-black solution. The final mixed solution was magnetically stirred at room temperature for 24 h and then centrifuged to obtain the blue-black substance. Finally, the resulting blue-black material was washed by centrifugation with acetone and ethanol sequentially for 3–5 times, then dried at 50 °C for 6 h to obtain the nanocomposite PEDOT: PSS/MWCNTs-COOH.

The blue-black solid prepared in the above steps was weighed and 1 mg mL^{-1} of Thi solution was added. The uniform blue-purple mixed solution after magnetic stirring for 2 h was the nanocomposite PEDOT: PSS/MWCNTs-COOH suspension used for electrode modification. Thi was added to provide redox sites in the electrochemical characterization process.

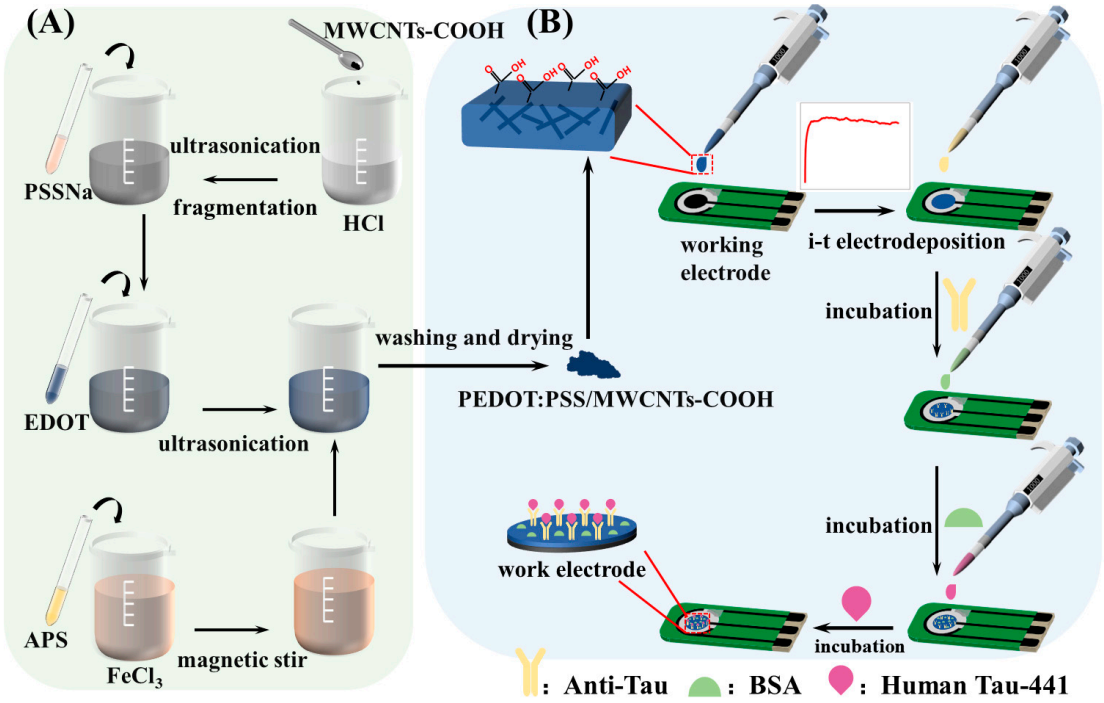

Figure 1. The illustration of proposed electrochemical immunosensor for Tau-441 detection based on PEDOT: PSS/MWCNTs-COOH. (**A**) The preparation of PEDOT: PSS/MWCNTs-COOH and (**B**) the fabrication and detection process of the proposed electrochemical immunosensor.

2.4. Fabrication of the Immunosensor

As shown in Figure 1B, with the optimized results of modified material concentration and deposition time, 4 mg mL^{-1} nanocomposite solution (covering the working electrode, reference electrode, and counter electrode simultaneously) was added dropwise to the electrode sheet, and then electrodeposition was performed in an electrochemical workstation using the current–time method (i-t), setting the initial potential parameter to −0.5 V, the sampling interval to 0.1 s and the running time to 200 s. After electrodeposition, the electrode was gently rinsed twice or three times with PBS solution (pH = 7.4) to remove modifying materials that were not electrodeposited onto the working electrode. Then, 6 µL of 0.05 mg mL^{-1} anti-Tau protein was added dropwise to the working electrode and incubated at 37 °C for 1 h. Based on the covalent bond fixation method, the chemical functional group (-COOH) of the modified material on the working electrode can be bound to-NH_2 of the Tau-441 antibody. After washing the electrode surface with PBS solution (pH = 7.4), 6 µL 1% BSA solution was added to the working electrode and incubated at 37 °C for 0.5 h. BSA can block the remaining active sites on the working electrode, preventing non-specific binding. Finally, the surface of the working electrode was cleaned with PBS solution (pH = 7.4) to remove the unbonded BSA, and dried at room temperature and placed at 4 °C for reserve. The immunosensor based on PEDOT: PSS/MWCNTs-COOH was constructed.

2.5. Electrochemical Measurements

The prepared immunosensor was incubated with 6.0 µL of different concentrations of Tau-441 for 0.5 h at 37 °C to ensure immunoreactivity between Tau protein and anti-Tau. Electrochemical measurements were performed at room temperature in 50 µL of 5 mmol L^{-1} $[Fe(CN)_6]^{3-/4-}$. CV was performed in the potential range of −0.5–0.8 V with a scan rate of 100 mV s^{-1}. DPV was performed in the potential range of −0.2–0.5 V with an amplitude of 0.05 V, a pulse width of 0.2 s, a sampling width of 0.02 s, and a pulse period of 0.5 s. The method was also applied to determine the linear range and samples under optimized experimental conditions.

3. Results and Discussion

3.1. Characterization of PEDOT: PSS/MWCNTs-COOH Nano-Composite

As shown in Figure 2A–C at different magnifications, the morphology indicates that the coarsely chopped polymers have a larger contact area, which helps them bond with other materials. The EDS elemental mapping images (Figure 2D) of PEDOT: PSS/MWCNTs-COOH nanocomposites show that the material contains S, C, O, and N. The analysis of the above results proved that the nanocomposites were successfully prepared. The EDS spectrum of the PEDOT: PSS/MWCNTs-COOH nanocomposite (Figure 3A) visually shows the weight percentage (*W*t%) and atomic percentage (*A*t%) of the elements contained. This indicates that the compound was successfully combined. The highest peak in the EDS spectrum (Figure 3A) is the silicon element because the nanocomposite was tested on silicon wafers.

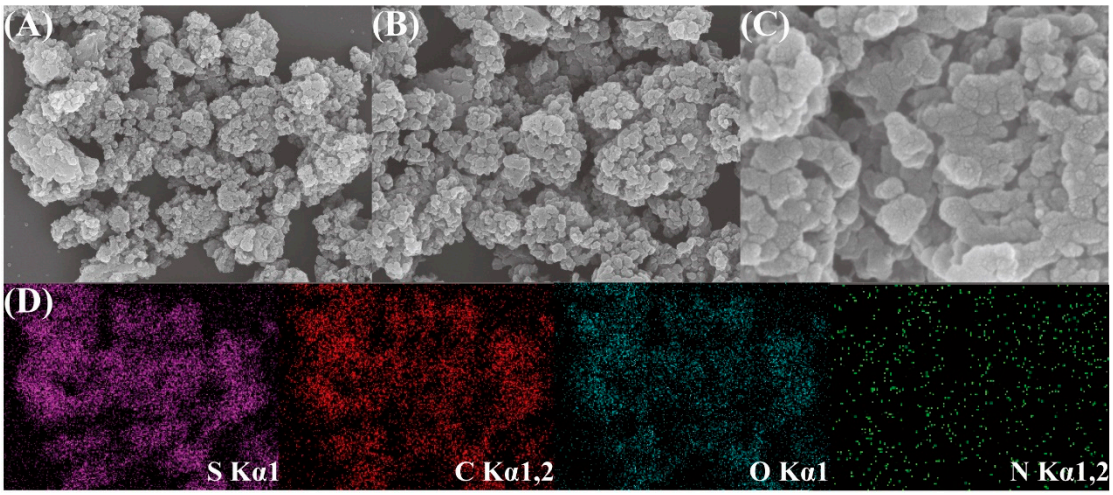

Figure 2. SEM images of PEDOT: PSS/MWCNTs-COOH nanocomposites in (**A**) 1 μm, (**B**) 500 nm and (**C**) 100 nm; (**D**) corresponding EDS elemental mapping images for S, C, O, N of PEDOT: PSS/MWCNTs-COOH nanocomposite.

The elemental analysis of the PEDOT: PSS/MWCNTs-COOH material was also performed using XPS to verify the successful synthesis of the nanocomposite. The elemental composition of the material is shown in Figure 3B. The peaks present in the spectrum represent four elements, O1s (532.5 eV), C1s (284.91 eV), S2p (163.32 eV), and N1s (399.23 eV) [37]. As shown in Figure 3C, the absorption peak in the UV diagram is within the wavelength range of 200–300 nm, and the absorption peak of the carboxyl group (-COOH) that plays the role of fixing the antibody in the prepared material is the same as the corresponding absorption peak in the figure, which indicates the feasibility of the material. FTIR (Figure 3D) spectral analysis further validates the successful preparation of the nanocomposites by the absorption peaks of the chemical bonds in specific organic functional groups. Curves a, b, and c correspond to the near-infrared optical absorption spectra of PEDOT: PSS, MWCNTs-COOH, and PEDOT: PSS/MWCNTs-COOH. The information on the chemical bonds is obtained through the different absorption frequencies in the plots, and the infrared data combined with the spectral library allows for qualitative analysis. In curve a, the peaks at 1349 cm^{-1}, 1122 cm^{-1}, 1070 cm^{-1}, and 974 cm^{-1} correspond to the stretching vibration of the PEDOT thiophene ring skeleton, the stretching vibration of the C-O-C chemical bond, the S=O vibrational stretching after PEDOT and PSSNa doping, and the vibrational stretching of the C-S bond on the thiophene ring, respectively. In curve b, the peak at about 3435 cm^{-1} corresponds to the broad peak of hydroxyl O-H stretching and the peak at 1705 cm^{-1} corresponds to the peak of carbonyl C=O stretching in carboxy COOH. In the FTIR spectrum of the PEDOT: PSS/MWNTs-COOH (curve c), in addition to the various characteristic absorption peaks of PEDOT: PSS, absorption peaks corresponding to the MWNTs-COOH phonon vibration and C=O stretching vibration appear at 3435 cm^{-1}

and 1647 cm^{-1} [38–40]. The absorption peak of curve c in the figure has the set of both curve a and curve b. Therefore, these results prove that the prepared material has the composite property of specific chemical bonding of the two materials and the composites were prepared successfully.

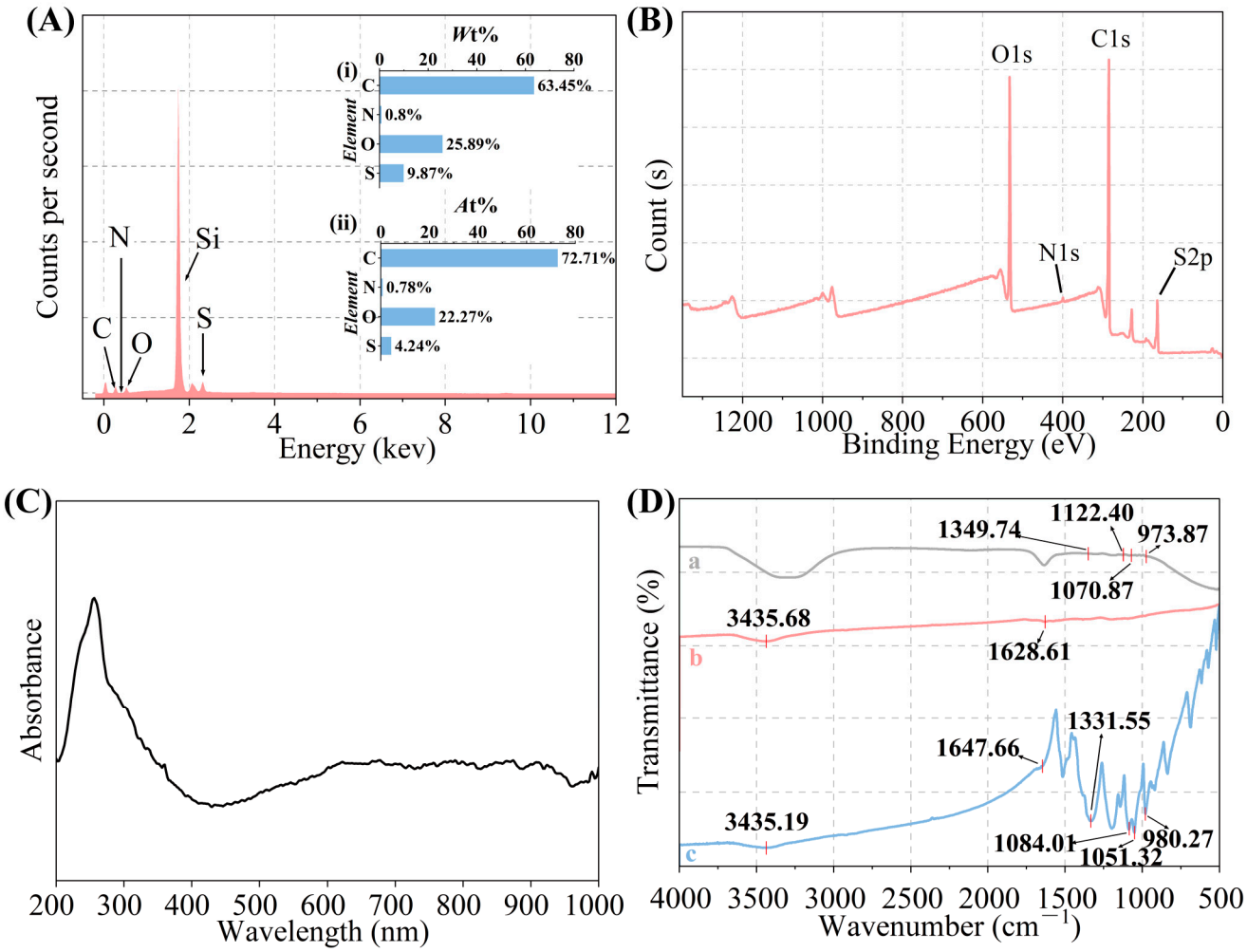

Figure 3. (**A**) The EDS spectrum of PEDOT: PSS/MWCNTs-COOH nanocomposite. Insert: the (i) *W*t% and (ii) *A*t% of PEDOT: PSS/MWCNTs-COOH; (**B**) XPS spectrum of PEDOT: PSS/MWCNTs-COOH; (**C**) UV spectrum of PEDOT: PSS/MWCNTs-COOH, and (**D**) FTIR spectrum of (a) PEDOT: PSS, (b) MWCNTs-COOH, and (c) PEDOT: PSS/MWCNTs-COOH.

3.2. Electrochemical Characterization of the Sensor

The surface of the working electrode after superimposed modification materials is shown in Figure 4A. The CV image of the bare working electrode shows a relatively small current peak (curve a). After the electrodeposition of PEDOT: PSS/MWCNTs-COOH, the peak current is significantly increased (curve b), which may be because the electrical conductivity of the working electrode can be greatly improved after modifying the nanocomposite material. Next, after antibody (curve c), BSA (curve d) and Tau-441 (curve e) were incubated in sequence on the working electrode, the redox current gradually decreased. This is because the antibody blocks electron transfer after covalently binding to the active group (-COOH), BSA is used to block the remaining active site on the working electrode to prevent non-specific adsorption, and the immune complex formed after incubating Tau-441 also hinders electron transfer. The experimental results are in accord with the analyses in theory. The experimental results of the current peak change are in good agreement with

the theoretical results of the expected immune sensor preparation, so it can be inferred that the immune sensor was successfully constructed.

The DPV measurements of electrodes modified with different materials are shown in Figure 4B. The variation in the current peaks, in Figure 4B, during the superposition of different modified materials is consistent with the CV measurements in Figure 4A. Compared with the bare electrode, the surface conductivity of the composite-modified working electrode was greatly improved, and gradually weakened after the gradual modification of antibody, BSA, and Tau-441. The results of the CV are shown in Figure 4C, and the curves of the working electrode at different scan rates after modifying with PEDOT: PSS/MWCNTs-COOH reveal positive correlation patterns. This result shows that the redox peaks gradually increase with the increase in scanning rate, and the absolute value of the current peak is positively correlated with the square root of the scanning rate. The linear relationship between the peak current and the square root of the scan rate (R^2 = 0.99 and 0.98) in Figure 4D indicates that the redox reaction on the electrode surface modified with PEDOT: PSS/MWCNTs-COOH is a diffusion-controlled process.

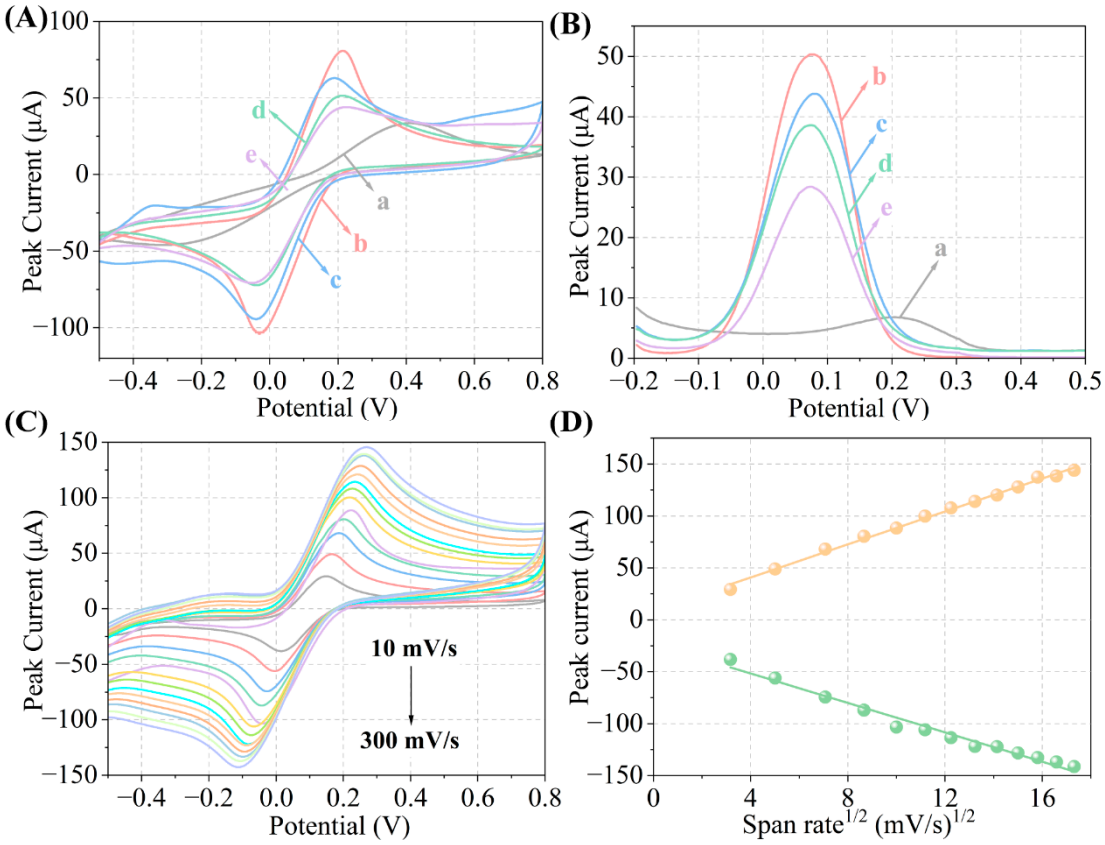

Figure 4. (**A**) CV and (**B**) DPV responses of (a) bare GCE, (b) GCE/PEDOT: PSS/MWCNTs-COOH, (c) GCE/PEDOT: PSS/MWCNTs-COOH/Anti-Tau, GCE/PEDOT: (d) PSS/MWCNTs-COOH/Anti-Tau/BSA, (e) GCE/PEDOT: PSS/MWCNTs-COOH/Anti-Tau/BSA/Tau-441. (**C**) CV responses of GCE/PEDOT: PSS/MWCNTs-COOH at different scan rates (10, 25, 50, 75, 100, 125, 150, 175, 200, 250, 225, 250, 275, 300 Mv s^{-1}) in 5 mM $[Fe(CN)_6]^{3-/4-}$ solution. (**D**) The linear relationship between the peak currents and the scan rate.

3.3. Optimization of Experimental Conditions

A variety of factors in the preparation of an immunosensor can affect the final detection results of the sensor. The preparation steps of the immunosensor were analyzed. The optimal conditions that came out to make the best performance of the sensor were selected as the final preparation scheme of the sensor. Firstly, the electrodeposition time of nanocomposite on the

working electrode is optimized. As can be seen from Figure S1A, the electrical conductivity of the working electrode gradually increases from 50–200 s, but begins to decline after the deposition time exceeds 200 s. Therefore, the best electrodeposition time is 200 s. The reason for this phenomenon may be that the electrodeposition time is too long, and the modification material accumulates too much on the surface of the working electrode to hinder the electron transfer efficiency. Then, the concentration of the modified material is further optimized. As can be seen from Figure S1B, under the condition that other conditions are consistent, when the concentration of the modified material is 4 mg mL^{-1}, the detection performance of the immune sensor is the best. The reason why the current change decreases after the concentration continues to increase may be that the thicker electrodeposited material hinders the conductive effect. Finally, since the specific recognition object of the prepared sensor is protein, the incubation process is very important for the performance of the sensor, so the incubation time and incubation temperature of Tau-441 were optimized. It can be seen from Figure S1C,D that the lowest peak current occurs at 37 °C when the incubation temperature is between 30 °C and 45 °C, and at 30 min when the incubation time is between 15 min and 60 min, the lowest peak current occurs at 30 min, which means that the antibody and antigen bind most under the above incubation conditions. Therefore, 37 °C and 30 min were selected as the incubation temperature and incubation time in the experiment.

3.4. Analytical Performance

Under the optimized conditions, the peak current of the prepared immunosensor through DPV at different Tau-441 concentrations 0, 0.01 ng mL^{-1}, 0.1 ng mL^{-1}, 1 ng mL^{-1}, 10 ng mL^{-1}, 0.1 µg mL^{-1}, 1 µg mL^{-1}, 10 µg mL^{-1}, 50 µg mL^{-1} in pH = 7.4 PBS changed, as shown in Figure 5A, indicating that the peak current gradually decreases with increasing antigen concentration. At a signal-to-noise ratio of 3, based on the antigen concentration and the corresponding current peak, the regression equation was $y = (1.39 \pm 0.07) \times \lg C_{tau\text{-}441} + (13.40 \pm 0.09)$ and $R^2 = 0.98$, as shown in Figure 5B. The detection range of this sensor is 0.00001–50 µg mL^{-1} and the detection limit is 0.0074 ng mL^{-1} using Equation (1). The formula for calculating detection limits is derived from the published literature [41]:

$$LOD = \frac{3SD_B}{Slope} = \frac{3SD_B}{\frac{dy}{dx}} = \frac{3SD_B}{\frac{dy}{d\ lnx} \times \frac{d\ lnx}{dx}} = \frac{3SD_B}{\frac{dy}{2.303(d\ logx)} \times \frac{1}{x}} = \frac{3(2.303)SD_B x}{\frac{dy}{d\ logx}} = \frac{3(2.303)SD_B x}{slope\ of\ the\ semilog\ plot} \quad (1)$$

where SD_B is standard deviation of blank; x is the limit of quantification or lowest concentration measured.

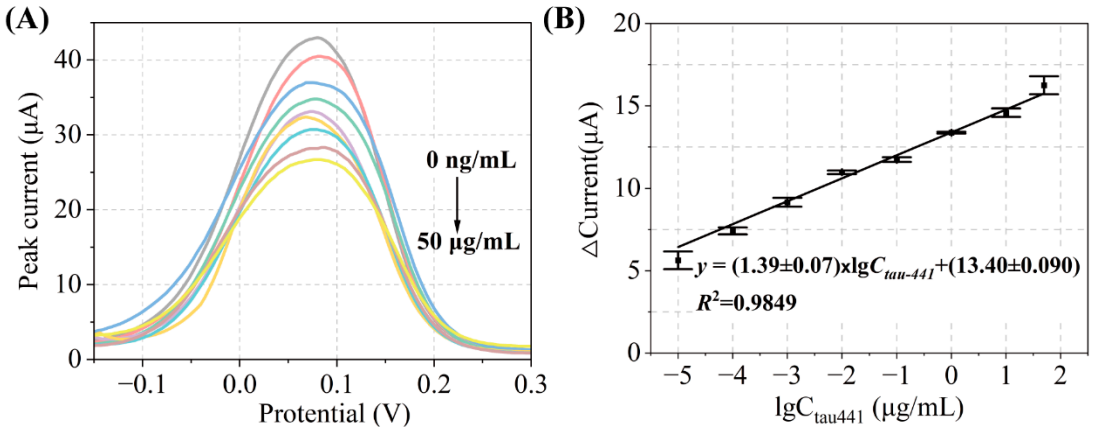

Figure 5. (**A**) DPV responses of the immunosensor incubated with different concentrations of Tau-441: 0, 0.01 ng mL^{-1}, 0.1 ng mL^{-1}, 1 ng mL^{-1}, 10 ng mL^{-1}, 0.1 µg mL^{-1}, 1 µg mL^{-1}, 10 µg mL^{-1}, and 50 µg mL^{-1}, in pH = 7.4 PBS (**B**) The linear relationship between the current response and the logarithm of the Tau-441 concentration.

The performance parameters of the immunosensor for the detection of Tau-441 protein reported in the literature are shown in Table 1. The detection limit of the developed sensor was not the lowest, but it had a wide detection range. Moreover, the immunosensor prepared in this experiment was relatively easy to prepare, not too difficult to detect and had relatively intuitive and direct detection results.

Table 1. Comparison of detection performance with different electrochemical immunosensors in Ref.

Biosensor	Electrochemical Techniques	LOD	Linear Range	Ref.
PDDA/G4 hydrogel	EIS, CV, DPV	1.31 pg mL^{-1}	0.01–100 ng mL^{-1}	[42]
MB@NAV	i-t	63 ng mL^{-1}	50–750 ng mL^{-1}	[43]
ITO/PET	DPV	4.3 ng mL^{-1}	5–100 ng mL^{-1}	[44]
Gold electrodes	EIS, CV, DPV	0.05 pM	0.05–3000 pM	[45]
Flower-shaped TiO_2	EIS	1.774 pg mL^{-1}	1–200 ng mL^{-1}	[46]
PEDOT:PSS/MWCNTs-COOH	CV, DPV	0.0074 ng mL^{-1}	0.00001–50 μg mL^{-1}	This work

3.5. Reproducibility, Specificity, and Stability of the Sensor

The reproducibility, specificity, and stability of the prepared immunosensor were evaluated using DPV, and the results of the assay are shown in Figure 6. For reproducibility, five groups of immunosensors were incubated with 0.01 ng mL^{-1} Tau-441 and the results are plotted as shown in Figure 6A, with a standard deviation of 0.40, which shows that the reproducibility of the immunosensor is good.

The selectivity of the sensor was evaluated by measuring the response currents of 10 μg mL^{-1} Tau-441 and blank, 50 μg mL^{-1} AFP, 50 μg mL^{-1} CEA, and 50 μg mL^{-1} BSA solution, and the mixture solution with the above concentrations, due to the presence of some proteins in the serum that interfere with the detection results. The experimental results are shown in Figure 6B. The immunosensor still has a high specificity when the concentration of the interfering agent is five times higher than the concentration of the detected marker.

To demonstrate the stability of the experiment, the immunosensor was stored under sealed conditions at 4 °C and taken out on the day of preparation for 1, 5, 10, 15, 20, and 25 days for the detection of 10 μg mL^{-1} Tau-441, respectively. Figure 6C shows a slight increase in the current, possibly due to the long storage time, reduced protein activity, and some impact on immune complex formation. But the change was not significant, indicating that the immune sensor has good stability.

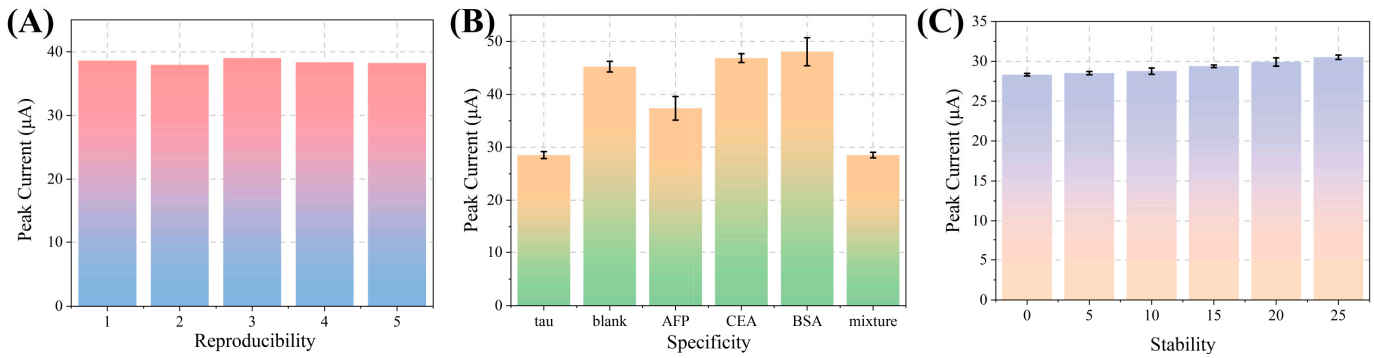

Figure 6. (**A**) Reproducibility of five immunosensors modified with 0.01 ng mL^{-1} Tau-441; (**B**) selectivity of the immunosensors with 10 μg mL^{-1} Tau-441 solution and blank solution, 50 μg mL^{-1} AFP solution, 50 μg mL^{-1} CEA solution and 50 μg mL^{-1} BSA solution, and the mixture solution with the above concentrations; and (**C**) stability of the immunosensors incubated with 10 μg mL^{-1} Tau-441 at 0, 5, 10, 15, 20, 25 days at 4 °C.

3.6. Real Sample Analysis

To evaluate the feasibility of the prepared immunosensor in practical application, different concentrations (0.01 ng mL^{-1}, 0.1 ng mL^{-1}, 1 ng mL^{-1}) of Tau-441 were added to the

normal human serum sample using the marked recovery method. Then, the concentration of the sample was detected by the immunosensor. As shown in Table 2, the recovery of the immunosensor ranged from 98.48% to 100.76%, and the RSD values ranged from 2.12% to 5.37%, indicating that the immunosensor prepared in this experiment has good potential for practical application.

Table 2. Determination of the recovery of Tau-441 in normal human serum with the prepared immunosensor (5 samples per group).

Sample	Added Amount (ng mL^{-1})	Found Amount (ng mL^{-1})	Recovery (%)	RSD (%)
1	0.01	0.009896	98.96	5.37
2	0.1	0.09848	98.48	2.12
3	1	1.10076	100.76	2.64

4. Conclusions

In this paper, an electrochemical immunosensor modified by PEDOT: PSS/MWCNTs-COOH was prepared for the label-free detection of Tau-441. The composite constructed using MWCNTs-COOH doped with PEDOT: PSS was modified on the working electrode, and its large specific surface area improved the electrical conductivity of the working electrode. The carboxylated group bond provided the binding site of the Tau-441 antibody protein, thus realizing the electrochemical immunodetection of Tau-441. Then, based on these, the constructed sensor achieved a low detection limit (0.0074 ng mL^{-1}) with a detection range of 0.00001 to 50 μg mL^{-1}. The immunosensor can provide a detection tool for Tau-441 for the early diagnosis of AD, simplify the preparation process, shorten the detection time and lower the operating threshold. In addition, the preparation process of the immunosensor modified by nano-composite materials is simple and has high conductivity. The preparation method of the sensor can be used as a reference for the immunodetection of various disease markers. The steps of multiple grooming and washing during the experiment also need to be simplified. Materials also need to be optimized to improve sensor performance and enable faster and more sensitive detection in future experiments.

Supplementary Materials: The following supporting information can be downloaded at: https://www.mdpi.com/article/10.3390/chemosensors11120573/s1, Figure S1: the effect of the (A) time of electrodeposition, (B) concentration of PEDOT: PSS/MWCNTs-COOH, (C) incubation temperature, and (D) incubation time on peak currents of the proposed immunosensor. Figure S2: element fitting diagram of XPS of PEDOT: PSS/MWCNTs-COOH (A) S, (B) C, (C) N and (D) O elements.

Author Contributions: H.R. was involved in manuscript writing, background investigation, experimental operation, and data management. X.L. contributed to the investigation. H.X. contributed to conceptualization and editing. S.W. participated in the review. F.Z. was involved in surveys and data management. Z.C. was involved in supervision, project management and capital acquisition. All authors have read and agreed to the published version of the manuscript.

Funding: This research was funded by the National Major Scientific Research Instrument and Equipment Development Project (61627807), Guangxi Science and Technology Major Special Project (2019AA12005), Project supported by the Joint Funds of the National Natural Science Foundation of China (U22A2092), Young Scientists Fund of the Guangxi Natural Science Foundation (2023GXNSFBA026075), and Guangxi Human Physiological Information Non Invasive Detection Engineering Technology Research Center Major Science and Technology Innovation Base Open Project (231001-K).

Institutional Review Board Statement: Not applicable.

Informed Consent Statement: Not applicable.

Data Availability Statement: The data of our study are available upon request.

Conflicts of Interest: The authors declare no conflict of interest.

References

1. Dubois, B.; Hampel, H.; Feldman, H.H.; Scheltens, P.; Aisen, P.; Andrieu, S.; Bakardjian, H.; Benali, H.; Bertram, L.; Blennow, K.; et al. Preclinical Alzheimer's disease: Definition, natural history, and diagnostic criteria. *Alzheimer's Dement.* **2016**, *12*, 292–323. [CrossRef]
2. Sexton, C.; Solis, M.; Aharon-Peretz, J.; Alexopoulos, P.; Apostolova, L.G.; Bayen, E.; Birkenhager, B.; Cappa, S.; Constantinidou, F.; Fortea, J.; et al. Alzheimer's disease research progress in the Mediterranean region: The Alzheimer's Association International Conference Satellite Symposium. *Alzheimer's Dement. J. Alzheimer's Assoc.* **2022**, *18*, 1957–1968. [CrossRef] [PubMed]
3. 2023 Alzheimer's disease facts and figures. *Alzheimers Dement.* **2023**, *19*, 1598–1695. [CrossRef]
4. Karaboga, M.N.S.; Sezgintürk, M.K. Analysis of Tau-441 protein in clinical samples using rGO/AuNP nanocomposite-supported disposable impedimetric neuro-biosensing platform: Towards Alzheimer's disease detection. *Talanta* **2020**, *219*, 121257. [CrossRef] [PubMed]
5. Bateman, R.J.; Barthelemy, N.R.; Benzinger, T.L.; Bollinger, J.G.; Fagan, A.M.; Gordon, B.A.; Hansson, O.; Holtzman, D.M.; Horie, K.; Li, M.; et al. Mass spectrometry measures of plasma Aβ, tau and P-tau isoforms' relationship to amyloid PET, tau PET, and clinical stage of Alzheimer's disease. *Alzheimer's Dement.* **2020**, *16*, e037518. [CrossRef]
6. Galvão, F.; Grokoski, K.C.; da Silva, B.B.; Lamers, M.L.; Siqueira, I.R. The amyloid precursor protein (APP) processing as a biological link between Alzheimer's disease and cancer. *Ageing Res. Rev.* **2019**, *49*, 83–91. [CrossRef]
7. Pimplikar, S.W. Reassessing the amyloid cascade hypothesis of Alzheimer's disease. *Int. J. Biochem. Cell Biol.* **2009**, *41*, 1261–1268. [CrossRef]
8. Muralidar, S.; Ambi, S.V.; Sekaran, S.; Thirumalai, D.; Palaniappan, B. Role of tau protein in Alzheimer's disease: The prime pathological player. *Int. J. Biol. Macromol.* **2020**, *163*, 1599–1617. [CrossRef]
9. 2021 Alzheimer's disease facts and figures. *Alzheimer's Dement. J. Alzheimer's Assoc.* **2021**, *17*, 327–406. [CrossRef]
10. Zhao, X.; Zeng, W.; Xu, H.; Sun, Z.; Hu, Y.; Peng, B.; McBride, J.D.; Duan, J.; Deng, J.; Zhang, B.; et al. A microtubule stabilizer ameliorates protein pathogenesis and neurodegeneration in mouse models of repetitive traumatic brain injury. *Sci. Transl. Med.* **2023**, *15*, eabo6889. [CrossRef]
11. Lo, C.H. Recent advances in cellular biosensor technology to investigate tau oligomerization. *Bioeng. Transl. Med.* **2021**, *6*, e10231. [CrossRef] [PubMed]
12. Lamontagne-Kam, D.; Ulfat, A.K.; Hervé, V.; Vu, T.-M.; Brouillette, J. Implication of tau propagation on neurodegeneration in Alzheimer's disease. *Front. Neurosci.* **2023**, *17*, 1219299. [CrossRef] [PubMed]
13. Sharma, A.; Angnes, L.; Sattarahmady, N.; Negahdary, M.; Heli, H. Electrochemical Immunosensors Developed for Amyloid-Beta and Tau Proteins, Leading Biomarkers of Alzheimer's Disease. *Biosensors* **2023**, *13*, 742. [CrossRef] [PubMed]
14. Bateman, R.J.; Barthelemy, N.R.; Benzinger, T.L.; Bollinger, J.G.; Fagan, A.M.; Gordon, B.A.; Hansson, O.; Holtzman, D.M.; Horie, K.; Li, M.; et al. CSF and blood plasma mass spectrometry measures of Aβ, tau, and NfL species and longitudinal relationship to preclinical and clinical staging of amyloid and tau aggregation and clinical stage of Alzheimer's disease. *Alzheimer's Dement.* **2021**, *17*, e050711. [CrossRef]
15. Taghdisi, S.M.; Danesh, N.M.; Ramezani, M.; Abnous, K. A novel M-shape electrochemical aptasensor for ultrasensitive detection of tetracyclines. *Biosens. Bioelectron.* **2016**, *85*, 509–514. [CrossRef]
16. Reddy, K.K.; Bandal, H.; Satyanarayana, M.; Goud, K.Y.; Gobi, K.V.; Jayaramudu, T.; Amalraj, J.; Kim, H. Recent Trends in Electrochemical Sensors for Vital Biomedical Markers Using Hybrid Nanostructured Materials. *Adv. Sci.* **2020**, *7*, 1902980. [CrossRef]
17. Khan, M.; Liu, X.; Tang, Y.; Liu, X. Ultra-sensitive electrochemical detection of oxidative stress biomarker 8-hydroxy-2′-deoxyguanosine with poly (L-arginine)/graphene wrapped Au nanoparticles modified electrode. *Biosens. Bioelectron.* **2018**, *117*, 508–514. [CrossRef]
18. Chen, J.; Song, N.; Zhang, N.; Gao, Z.; Wu, D.; Hongmin, M.; Ren, X.; Wei, Q. Smartphone-controlled portable photoelectrochemical immunosensor for point-of-care testing of carcinoembryonic antigen. *Chem. Eng. J.* **2023**, *473*, 145276. [CrossRef]
19. Zhou, T.; Ji, W.; Fan, H.; Zhang, L.; Wan, X.; Fan, Z.; Liu, G.L.; Peng, Q.; Huang, L. A Metasurface Plasmonic Analysis Platform Combined with Gold Nanoparticles for Ultrasensitive Quantitative Detection of Small Molecules. *Biosensors* **2023**, *13*, 681. [CrossRef]
20. Wu, Y.; Fu, Y.; Guo, J.; Guo, J. Single-molecule immunoassay technology: Recent advances. *Talanta* **2023**, *265*, 124903. [CrossRef]
21. Wang, D.; Chen, Y.; Xiang, S.; Hu, H.; Zhan, Y.; Yu, Y.; Zhang, J.; Wu, P.; Liu, F.Y.; Kai, T.; et al. Recent advances in immunoassay technologies for the detection of human coronavirus infections. *Front. Cell. Infect. Microbiol.* **2023**, *12*, 1040248. [CrossRef] [PubMed]
22. Scarano, S.; Lisi, S.; Ravelet, C.; Peyrin, E.; Minunni, M. Detecting Alzheimer's disease biomarkers: From antibodies to new bio-mimetic receptors and their application to established and emerging bioanalytical platforms—A critical review. *Anal. Chim. Acta* **2016**, *940*, 21–37. [CrossRef] [PubMed]
23. Loeffler, D.A.; Klaver, A.C.; Coffey, M.P. ELISA measurement of specific antibodies to phosphorylated tau in intravenous immunoglobulin products. *Int. Immunopharmacol.* **2015**, *28*, 1108–1112. [CrossRef] [PubMed]
24. Špringer, T.; Hemmerová, E.; Finocchiaro, G.; Krištofiková, Z.; Vyhnálek, M.; Homola, J. Surface plasmon resonance biosensor for the detection of tau-amyloid β complex. *Sens. Actuators B Chem.* **2020**, *316*, 128146. [CrossRef]
25. Rezabakhsh, A.; Rahbarghazi, R.; Fathi, F. Surface plasmon resonance biosensors for detection of Alzheimer's biomarkers; an effective step in early and accurate diagnosis. *Biosens. Bioelectron.* **2020**, *167*, 112511. [CrossRef] [PubMed]
26. Nangare, S.; Patil, P. Poly(allylamine) coated layer-by-layer assembly decorated 2D carbon backbone for highly sensitive and selective detection of Tau-441 using surface plasmon resonance biosensor. *Anal. Chim. Acta* **2023**, *1271*, 341474. [CrossRef] [PubMed]

27. Razzino, C.A.; Serafín, V.; Gamella, M.; Pedrero, M.; Montero-Calle, A.; Barderas, R.; Calero, M.; Lobo, A.O.; Yáñez-Sedeño, P.; Campuzano, S.; et al. An electrochemical immunosensor using gold nanoparticles-PAMAM-nanostructured screen-printed carbon electrodes for tau protein determination in plasma and brain tissues from Alzheimer patients. *Biosens. Bioelectron.* **2020**, *163*, 112238. [CrossRef]
28. Song, Y.; Xu, T.; Zhu, Q.; Zhang, X. Integrated individually electrochemical array for simultaneously detecting multiple Alzheimer's biomarkers. *Biosens. Bioelectron.* **2020**, *162*, 112253. [CrossRef]
29. Wong, A.; Santos, A.M.; Fatibello-Filho, O. Simultaneous determination of paracetamol and levofloxacin using a glassy carbon electrode modified with carbon black, silver nanoparticles and PEDOT:PSS film. *Sens. Actuators B Chem.* **2018**, *255*, 2264–2273. [CrossRef]
30. Yola, B.B.; Karaman, C.; Özcan, N.; Atar, N.; Polat, I.; Yola, M.L. Electrochemical Tau Protein Immunosensor Based on MnS/GO/PANI and Magnetite-incorporated Gold Nanoparticles. *Electroanalysis* **2022**, *34*, 1519–1528. [CrossRef]
31. Ben Hassine, A.; Raouafi, N.; Moreira, F.T. Novel biomimetic Prussian blue nanocubes-based biosensor for Tau-441 protein detection. *J. Pharm. Biomed. Anal.* **2023**, *226*, 115251. [CrossRef] [PubMed]
32. Keshmiri, N.; Hoseini, A.H.A.; Najmi, P.; Liu, J.; Milani, A.S.; Arjmand, M. Highly conductive polystyrene/carbon nanotube/PEDOT:PSS nanocomposite with segregated structure for electromagnetic interference shielding. *Carbon* **2023**, *212*, 118104. [CrossRef]
33. Hou, S.; Chen, H.; Lv, D.; Li, W.; Liu, X.; Zhang, Q.; Yu, X.; Han, Y. Highly Conductive Inkjet-Printed PEDOT:PSS Film under Cyclic Stretching. *ACS Appl. Mater. Interfaces* **2023**, *15*, 28503–28515. [CrossRef]
34. Okpalugo, T.; Papakonstantinou, P.; Murphy, H.; McLaughlin, J.; Brown, N. High resolution XPS characterization of chemical functionalised MWCNTs and SWCNTs. *Carbon* **2005**, *43*, 153–161. [CrossRef]
35. Wu, H.; Zhang, G.; Yang, X. Electrochemical immunosensor based on Fe_3O_4/MWCNTs-COOH/AuNPs nanocomposites for trace liver cancer marker alpha-fetoprotein detection. *Talanta* **2023**, *259*, 124492. [CrossRef] [PubMed]
36. Zhang, Z.; Chen, G.; Wang, H.; Li, X. Template-Directed In Situ Polymerization Preparation of Nanocomposites of PEDOT:PSS-Coated Multi-Walled Carbon Nanotubes with Enhanced Thermoelectric Property. *Chem. Asian J.* **2015**, *10*, 149–153. [CrossRef]
37. Lien, S.-Y.; Lin, P.-C.; Chen, W.-R.; Liu, C.-H.; Lee, K.-W.; Wang, N.-F.; Huang, C.-J. The Mechanism of PEDOT: PSS Films with Organic Additives. *Crystals* **2022**, *12*, 1109. [CrossRef]
38. Sayyad, P.W.; Sontakke, K.S.; Farooqui, A.A.; Shirsat, S.M.; Tsai, M.-L.; Shirsat, M.D. A novel three-dimensional electrochemical Cd(II) biosensor based on l-glutathione capped poly(3,4-ethylenedioxythiophene):polystyrene sulfonate/carboxylated multiwall CNT network. *J. Sci. Adv. Mater. Devices* **2022**, *7*, 100504. [CrossRef]
39. Wu, R.; Xu, X.; Li, N.; Liu, C.; Chen, X.; Chen, Z.; Lan, X.; Jiang, Q.; Xu, J.; Jiang, F.; et al. Ultralong-Cycling and Free-Standing Carboxylated Graphene/PEDOT:PSS Films as Electrode for Flexible Supercapacitors. *Int. J. Energy Res.* **2023**, *2023*, 5695694. [CrossRef]
40. Chen, T.; Chen, Q.; Liu, G.; Chen, G. High cycling stability and well printability poly(3,4-ethylenedioxythiophene):poly(styrene sulfonate)/multi-walled carbon nanotube nanocomposites via in situ polymerization applied on electrochromic display. *J. Appl. Polym. Sci.* **2018**, *135*, 45943. [CrossRef]
41. Mahato, K.; Purohit, B.; Bhardwaj, K.; Jaiswal, A.; Chandra, P. Novel electrochemical biosensor for serotonin detection based on gold nanorattles decorated reduced graphene oxide in biological fluids and in vitro model. *Biosens. Bioelectron.* **2019**, *142*, 111502. [CrossRef] [PubMed]
42. Chen, Q.; Hu, J.; Mao, Z.; Koh, K.; Chen, H. Loach mucus-like guanosine-based hydrogel as an antifouling coating for electrochemical detection of tau protein. *Sens. Actuators B Chem.* **2022**, *370*, 132419. [CrossRef]
43. Toyos-Rodríguez, C.; Llamedo-González, A.; Pando, D.; García, S.; García, J.; García-Alonso, F.; de la Escosura-Muñiz, A. Novel magnetic beads with improved performance for Alzheimer's disease biomarker detection. *Microchem. J.* **2022**, *175*, 107211. [CrossRef]
44. Toyos-Rodríguez, C.; García-Alonso, F.J.; de la Escosura-Muñiz, A. Towards the maximization of nanochannels blockage through antibody-antigen charge control: Application for the detection of an Alzheimer's disease biomarker. *Sens. Actuators B Chem.* **2023**, *380*, 133394. [CrossRef]
45. Shiravandi, A.; Yari, F.; Tofigh, N.; Ashtiani, M.K.; Shahpasand, K.; Ghanian, M.-H.; Shekari, F.; Faridbod, F. Earlier Detection of Alzheimer's Disease Based on a Novel Biomarker *cis* P-tau by a Label-Free Electrochemical Immunosensor. *Biosensors* **2022**, *12*, 879. [CrossRef]
46. Zhang, Z.-H.; Hu, J.; Zhu, H.; Chen, Q.; Koh, K.; Chen, H.; Xu, X.-H. A facile and effective immunoassay for sensitive detection of phosphorylated tau: The role of flower-shaped TiO_2 in specificity and signal amplification. *Sens. Actuators B Chem.* **2022**, *366*, 132015. [CrossRef]